Rheol Acta
DOI 10.1007/s00397-007-0206-7

ORIGINAL CONTRIBUTION

Rheometric and rheo-optical investigation on the effect of the aliphatic chain length of the surfactant on the shear thickening of dilute worm-like micellar solutions

Jalal Dehmoune · Jean-Paul Decruppe · Olivier Greffier · Hong Xu

Received: 23 December 2006 / Accepted: 30 April 2007

Abstract In this study, a new way of understanding the shear-thickening phenomenon in self-assembled solutions is introduced. The near- and out-of-equilibrium behavior is investigated in four aqueous micellar solutions containing surfactants of the same family: the alkyltrimethylammonium bromide mixed with an ionic salt at equimolar concentration. Thus, the four molecules of surfactants have the same polar head but different aliphatic chain length containing 12, 14, 16, and 18 carbon atoms. In aqueous solutions, the attractive forces between the surfactant molecules depend on the length of the aliphatic chain, thus, varying this parameter will have a definite influence on the aggregation number, the shape and dimension of the micelles. According to our results, the evolution of the low shear viscosity is affected by the chain length. The rheometric measurements performed in steady and time-dependent flows show that the emergence, the range, and the amplitude of the shear thickening also depend on this parameter. However, in the domain of high shear rates, after reaching the maximum of viscosity, all flow curves superimpose irrespective of the chain length. The rheo-optic measurements confirm the apparition of the shear-induced structure (SIS); this new phase is locally oriented and the chain length affects strongly the micelles orientation and the birefringence intensity. These results undoubtedly demonstrate that the chain length plays an important role in the behavior near equilibrium and under shear flow of the micellar systems.

Keywords Shear-induced structure · Couette flow · Strain- and stress-controlled modes · Stationary flow · Rheometry · Rheo-optic

Introduction

Surfactants are met in many industrial fields like food, cosmetics, or paint industries. These molecules are built with two antagonistic parts: a polar head that appreciates being surrounded by water molecules and a hydrophobic aliphatic chain. Because of this dual character, the individual molecules will self-assemble into micelles of various shapes under specific thermodynamical conditions. In the domain of dilute concentrations, the shape asymmetry of the micelles is rather weak: the particles are spheres or small cylinders. However, despite these simple shapes, some aqueous solutions pertaining to this domain will exhibit unusual behavior under the action of an hydrodynamic field. When subjected to increasing shearing conditions, the apparent viscosity will suddenly start to increase; this is the shear-thickening transition widely observed in literature (Rehage and Hoffmann 1982, 1988; Hu et al. 1994, 1998a, b; Liu and Pine 1996; Gamez-Corrales et al. 1999). Its amplitude is found to be the highest when specific conditions in the choice of the samples are met : the micellar concentration must be in the dilute regime where the micelles are nearly or weakly entangled (Rehage and Hoffmann 1982, 1988; Hoffmann et al. 1991a, b; Hu et al. 1994; Liu and Pine 1996), the ratio of the surfactant concentration to the counterion concentra-

Paper presented at the third Annual European Rheology Conference (AERC 2006) on April 27–29, 2006, Crete, Greece.

J. Dehmoune · J.-P. Decruppe (✉) · O. Greffier · H. Xu
Laboratoire de Physique des Milieux Denses,
Groupe des Fluides Complexes, IPEM,
1 Bd. F. Arago,
57078 Metz, France
e-mail: decruppe@univ-metz.fr

tion must equal the unity (Hu et al. 1994), and finally, the counterion should be the anion of an organic salt like sodium salicylate with the surfactant studied in this work (Hartmann 1997; Hu et al. 1994; Liu and Pine 1996). Previous works agree in explaining the viscosity increase by the emergence of a shear-induced structure (SIS; Rehage and Hoffmann 1982, 1988; Liu and Pine 1996; Hu et al. 1998a, b; Boltenhagen et al. 1997), resulting from a transition to a gel phase (Rehage and Hoffmann 1982, 1988; Wunderlich et al. 1987; Liu and Pine 1996; Boltenhagen et al. 1997). A direct observation of the gap shows that the turbid SIS coexists with a fluid phase (Liu and Pine 1996; Boltenhagen et al. 1997; Hu et al. 1998a, b). But the main controversy still lies in the nature and the structure of the SIS. It is a reversible phase containing, according to different theories, supramolecules resulting from a fusion mechanism (Rehage and Hoffmann 1982, 1988; Wunderlich et al. 1987; Liu and Pine 1996; Boltenhagen et al. 1997; Hu et al. 1998a, b), long micelles oriented in the flow direction (Rehage et al. 1986; Wunderlich et al. 1987) and stacked in a pseudo-nematic phase (Hoffmann et al. 1991b), microscopic aggregates of a sponge phase (Hoffmann et al. 1991a; Liu and Pine 1996), or necklaces of oriented micelles rings (Hoffmann et al. 1991b).

Despite all these efforts, little information concerning the growth and the composition of the SIS is reliable. The lack of agreement between these previous works can be imputed to various causes such as the different chemical composition of the surfactant, the concentration or the nature of the counterion, and the various shearing devices or rheometers. The main goal of this experimental work consists in bringing new information concerning the shear-thickening transition by introducing the length of the aliphatic chain effect as the main parameter of this study.

This choice is dictated by the fact that in aqueous solution, the aliphatic hydrophobic chain is at the origin of the attractive forces between molecules. To find out the importance of this parameter, dilute micellar solutions are prepared with surfactant molecules belonging to the same family: the alkyltrimethylammonium bromide; four molecules having 12, 14, 16, and 18 carbon atoms in the tail and the same polar head are chosen; C_{16}TAB is well known and has already been widely studied we quote especially the works of Liu and Pine (1996) and Hu et al. (1994). However, less information or even none can be found on the flow behavior of C_{12}-, C_{14}-, and C_{18}TAB. In this paper, we report and describe experimental results, i.e., zero shear viscosity, stationary flow curves under stress- and strain-controlled modes of a new surfactant class not yet explored in the literature. We performed steady shear flow measurements of the extinction angle and of the birefringence intensity in the same flow conditions as in rheometry.

Experiments

Materials

The decyltrimethylammonium bromide (C_{12}TAB or $CH_3(CH_2)_{11}N(CH_3)_3^+Br^-$) and myristyltrimethylammonium bromide (C_{14}TAB or $CH_3(CH_2)_{13}N(CH_3)_3^+Br^-$) are chemicals from Acros Organics, while cetyltrimethylammonium bromide (C_{16}TAB or $CH_3(CH_2)_{15}N(CH3)_3^+Br^-$), octadecyltrimethylammonium bromide (C_{18}TAB, $CH_3(CH_2)_{17}N(CH_3)_3^+Br^-$), as well as sodium salicylate (NaSal), come from Aldrich. They are used as bought without any further treatment or purification. The way the solutions are prepared is quite simple: carefully weighted (with a precision of $\pm 10^{-4}$ g) amounts of each surfactant are mixed in distilled water with the necessary amount of NaSal to make an equimolar solution. The role played by the salt is well known: it acts as a co-surfactant that creeps in between the polar heads; thus, the repulsive interactions are screened and the micelles increase in length.

Devices

Three different rheometers were used during this experimental campaign; they were all equipped with the same measuring device: a Couette cell. In the strain-controlled rheometer RFS III (TA Instruments), the inner cylinder is attached to the stress gauge and the outer one is rotating at a constant angular velocity; the AR 2000 (from the same manufacturer) works in stress-controlled mode with the rotor being, this time, the inner cylinder. Simultaneous to rheology, flow birefringence experiments were performed on a home-built bench (Decruppe et al. 1989); this technique allows the measurement of the extinction angle and the birefringence intensity under controlled strain in a Couette cell. In both cases, the cylinders form a 1-mm gap but the curvature is different. For the solutions having the lowest concentration (1 mM), a low shear viscosimeter LS30 (Contraves) is well adapted to the 1-mM solutions. During all the experiments, the temperature is kept constant at 23±0.3 °C with a circulating water bath.

Results and discussion

Steady-state flow curves for various concentrations

The rheological characterization of the systems C_nTAB was performed under steady-state conditions. When working with viscoelastic fluids, drawing the flow curves or the viscosity curves will reveal the general rheological behavior of the system. They are displayed in Fig. 1 where the variation of the apparent viscosity η appear as a function of

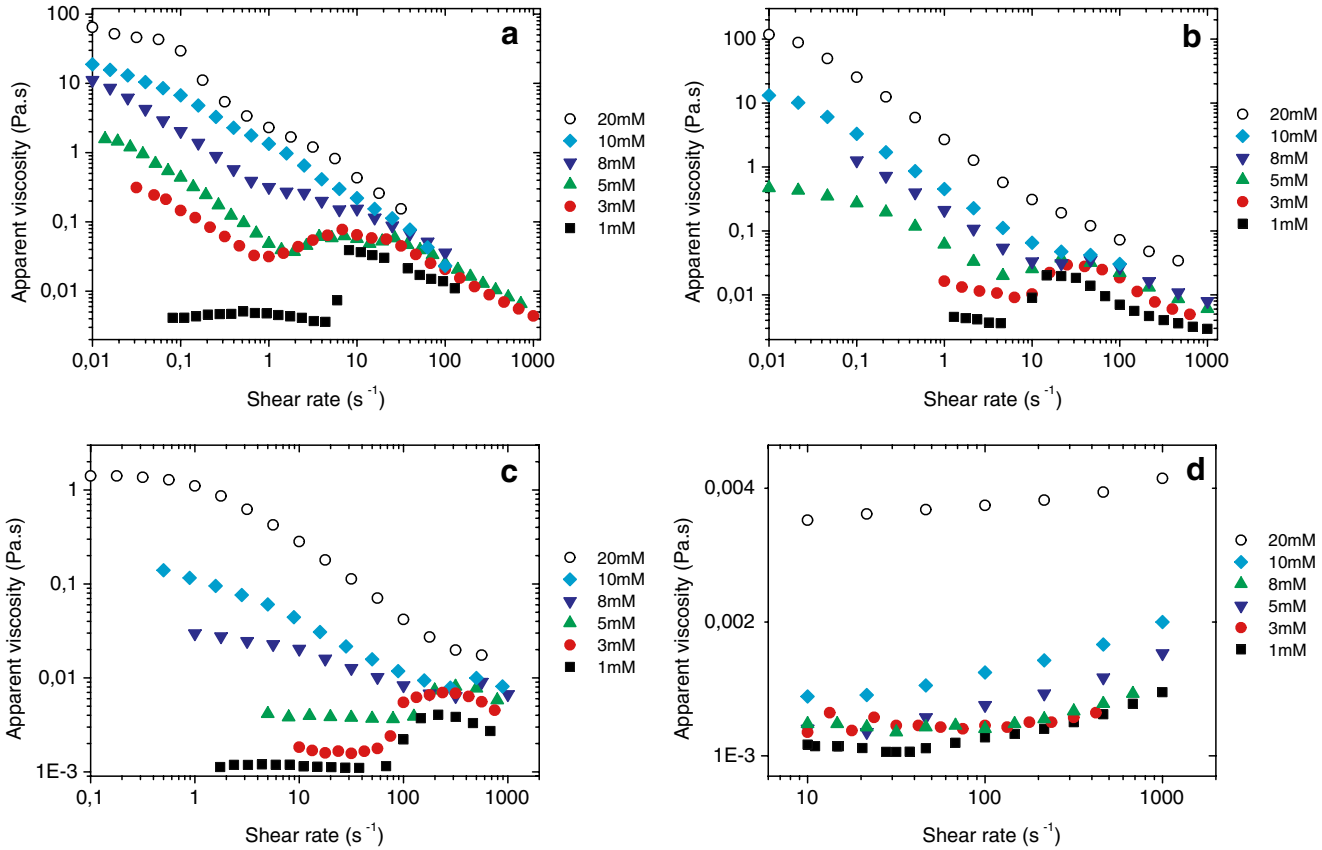

Fig. 1 Variation of the apparent viscosity as a function of the shear rate for various surfactants solutions C_{18}TAB (**a**), C_{16}TAB (**b**), C_{14}TAB (**c**), and C_{12}TAB (**d**) at different concentrations

the shear rate $\dot{\gamma}$ for samples with different surfactant concentrations. The measurements are recorded in strain-controlled mode, 600 s after the inception of the flow; this duration will represent the steady flow behavior at a given state.

The set of curves in Fig. 1 gives an overall view of the part played by the concentration and by the chain length on the flow behavior and, in particular, on the shear-thickening transition. Except for the system C_{12}TAB that always has a nearly Newtonian behavior (see Fig. 1d), the viscosity curves of the three other surfactants are qualitatively similar with a marked increase of the viscosity; common characteristics are found between them—they all confirm that shear thickening only occurs when the concentration of the detergent (C_D) is small: 5 mM or less. In that case, before the shear-thickening transition when ($\dot{\gamma} < \dot{\gamma}_c$), the solution is either shear thinning or Newtonian at C_D=1 mM. Going from a newtonian behavior to a shear-thinning one reveals that the shape of the micelles has changed from a particle having a nearly spherical symmetry (sphere) to an asymmetrical shape (cylinder of elongated ellipsoid) sensitive to the orientating action of the hydrodynamic field.

Another general characteristic of a shear-thickening curve already mentioned by Gamez-Corrales et al. (1999) arises from our experiments; a viscosity curve $\eta\left(\dot{\gamma}\right)$ appears as made of three parts. They will be denoted as regimes I, II, and III according to the shear rate ranges they cover; thus, *regime I* comes before the shear thickening transition, *regime II* corresponds to the increasing part of the viscosity curve, and finally, *regime III* is the remaining part extending after the maximum in the $\eta\left(\dot{\gamma}\right)$ curve. It seems important to us to introduce another region that represents the behavior at low shear rates. This part is the *near-equilibrium regime*. We shall successively examine the behavior of the fluid samples in these regimes.

Near-equilibrium regime. The low shear viscosity η_0 is an important characteristic of micellar solutions near equilibrium; it can easily be found by extrapolating the viscosity curves $\eta\left(\dot{\gamma}\right)$ (see Fig. 1) to null shear rate. The variations of the low shear viscosity are then drawn vs. the surfactant concentration for the various chain lengths (see Fig. 2); this is a way to find the concentration C^* that separates the dilute regime from the semi-dilute one; it can also bring information on the range of concen-

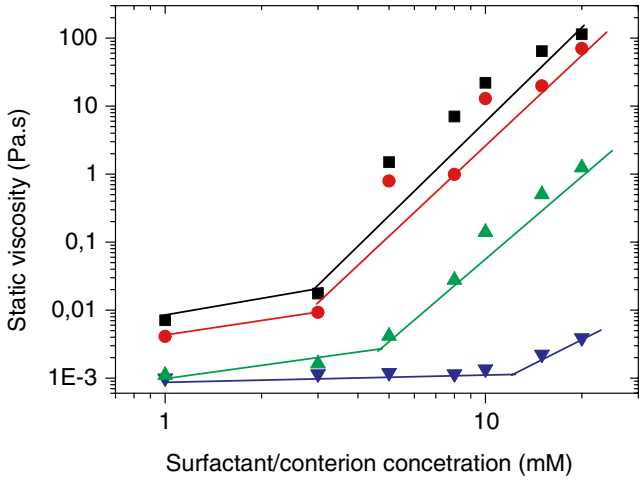

Fig. 2 Low shear viscosity vs concentration of surfactant solutions with various chain lengths C_{18}TAB (*square*), C_{16}TAB (*circle*), C_{14}TAB (*triangle*), and C_{12}TAB (*inverted triangle*); the lines are a guide to the eye

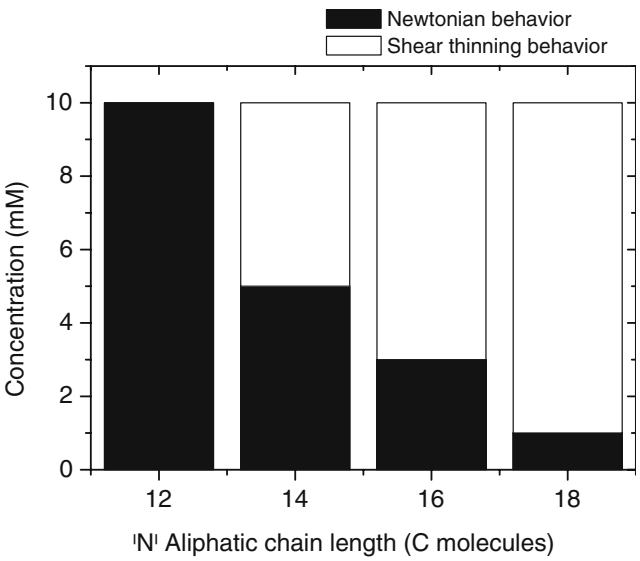

Fig. 3 The type of flow behavior in regime I (before the shear thickening transition) as function of to the chain length and the concentration

trations where SIS can be observed (Wunderlich et al. 1987; Hoffmann et al. 1991a, b). The overall behavior of η_0 is as expected; in the low concentration range, the static viscosity is close to the solvent viscosity; for example, with a 1 mM concentration, solutions C_{12}TAB, C_{14}TAB, C_{16}TAB, and C_{18}TAB have a static viscosity respectively of 1, 1.1, 4.1, and 7.1 times that of the solvent. These systems belong to the dilute regime that is characterized by high amplitude of the shear-thickening phenomenon. The limits of the dilute regime will vary from one system to another. The curves $\eta_0\left(\dot{\gamma}\right)$ appear as made of two nearly straight segments the intersection of which leads to the concentration C^*; the transition between the dilute and the semi-dilute regime is marked by a sharp growth of the low shear viscosity, which is the sign of entanglements of the micelles in the fluids; this transition is easily seen for C_{12}TAB, C_{14}TAB, C_{16}TAB, and C_{18}TAB. We notice that this critical concentration decreases when the surfactant chain length increases; this evolution is explained by the larger volume occupied by the long chain compared to the shorter ones; a large volume will make the formation of micelles at low concentration easier.

Regime I (before the shear-thickening transition) The different flow types before the shear-thickening transition are gathered in Fig. 3; it is a bar diagram with the number of carbon atoms 'N' in the chain on the *x*-axis and the surfactant concentration C_D on the *y*-axis. The Newtonian behavior occurs for small values of C_D and of the chain length. A C_{12}TAB/NaSal solution does not exhibit shear thickening and behaves like Newtonian fluid all over the explored concentrations. When 'N' increases, the limit between an empty rectangle (shear-thinning behavior) and a black one (Newtonian fluid) decreases, and a C_{18}TAB/NaSal system will already have a shear-thinning behavior beyond a 1-mM concentration.

A Newtonian plateau is the sign of freely rotating micelles without entanglement (Wunderlich et al. 1987; Hoffmann et al. 1991a, b). However, a 3-mM C_{14}TAB/NaSal solution shows flow birefringence (see "Rheo-optical flow under controlled shear rate") in the Newtonian domain; this is an indication that the micelles have an asymmetrical shape (probably small cylinders); for longer chain length (C_{16} and C_{18}) at C_D=3 mM, the flow is shear thinning before the shear-thickening transition; the increasing shearing conditions is inducing a disentanglement and an alignment of the long micelles in the flow direction is offering less resistance to the flow. In a partial conclusion, we can state that the aliphatic chain length has as strong effect on the intermicellar arrangement.

Regime II (shear-thickening domain) Figure 4 displays the shear-thickening amplitude as a function of the concentration C_D it is the ratio of the apparent viscosity maximum to the viscosity recorded before the beginning of the transition. In the low concentration range (C_D=1 mM), the amplitude of the maximum decreases with '*N*', a turn-over happens at C_D=3 mM, and C_{18}TAB has now the smallest amplitude. When C_D is further increased, the three curves tend to superimpose with the shear thickening disappearing at first for C_{18}TAB, then C_{16}TAB, and finally, C_{14}TAB at C_D=10 mM. The combination of the results displayed in Figs. 3 and 4 allows us to think that the properties of the shear-thickening phenomenon strongly depend on the type

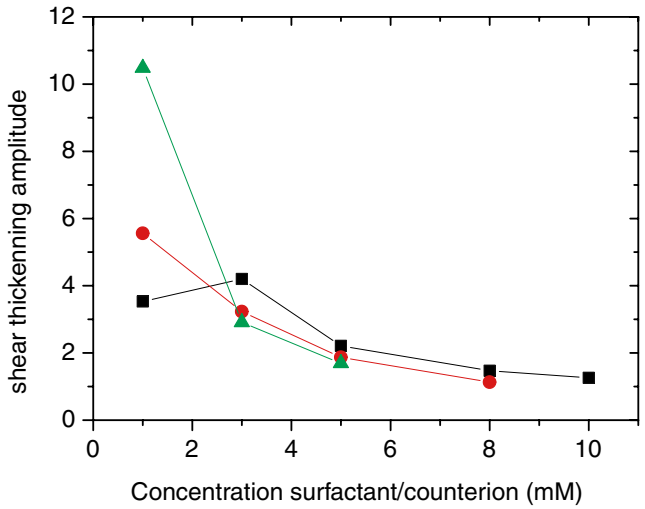

Fig. 4 Evolution of the shear thickening amplitude vs the concentration of the surfactant systems C_{18}TAB (*square*), C_{16}TAB (*circle*), and C_{14}TAB (*triangle*)

and history of the flow in domain I. A shear-thinning behavior in region I will give smaller amplitude than a Newtonian solution would [see, for example, Fig. 1a, the viscosity curves corresponding to C_D=1 mM (black squares) and to C_D=3 or 5 mM (full circles and triangles)]. No shear thickening is found with C_{12}TAB in the shear rates range (whatever the concentration C_D). It should be emphasized that the shear-thickening phenomenon extends over a shorter range when the flow in region I is newtonian than when it has a viscoelastic character. Thus, the entanglements interfere with the SIS formation mechanism. The critical shear rates at the emergence of the shear thickening are easily deduced from the viscosity curves in Fig. 1. These values are plotted as a function of the chain length '*N*'. By looking at Fig. 5, we will observe that increasing the chain length leads to a smaller critical shear rate $\dot{\gamma}_c$ and, for any surfactant, increasing the concentration results in increasing $\dot{\gamma}_c$.

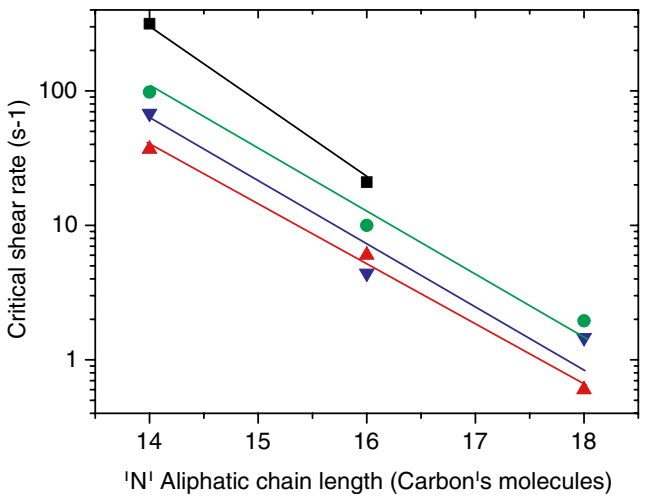

Fig. 5 Critical shear rate vs aliphatic chain length for different concentrations: 8 mM (*square*), 5 mM (*circle*), 3 mM (*triangle*), and 1 mM (*inverted triangle*); the lines are a guide to the eye

Regime III (shear-thinning flow) For all the surfactants, the flow now becomes shear thinning and for a given surfactant, all the curves tend to superimpose at high shear rates (see, for example, Fig. 1a). It is assumed that the SIS breaks down and disintegrates (Wunderlich et al. 1987; Hoffmann et al. 1991a; Liu and Pine 1996; Hu et al. 1998a, b) but our results do not agree with theirs (see "Rheo-optical flow under controlled shear rate") because an oriented structure remains even at high shear rates.

Rheological behaviour of the 3-mM solutions

The solutions at 3 mM are subjected to shear under strain- and stress-controlled modes. Particular attention is given to this concentration for several reasons; the 3-mM concentration is close to the critical micellar concentration (CMC). Except for C_{12}TAB (Basu Ray et al. 2005), the micelles are cylindrical, and the shear-thickening amplitude is important (Hoffmann et al. 1991a, b; Wunderlich et al. 1987; see Fig. 2); indeed the sodium salicylate counterion makes the CMC decrease (Swanson-Vethamuthu et al. 1996).

Steady state flow in strain-controlled mode

The shear stress σ and the apparent viscosity η are plotted vs the shear rate $\dot{\gamma}$ (see Fig. 6) with the chain length as a variable parameter. The three regions in the viscosity evolution mentioned before clearly appear on Fig. 6b: The Newtonian or shear-thinning flow followed by the shear-thickening region and, finally, a shear-thinning phase. The comparison at a given concentration clearly reveals the role of the aliphatic chain length on each regime.

From Fig. 6, we can describe the stationary flow behavior in the three regions for the three chain lengths:

- Regime I (before the shear-thickening transition): in the low shear rates range ($\dot{\gamma} < \dot{\gamma}_c$), C_{12}TAB and C_{14}TAB are newtonian with a viscosity, respectively of 1.1 and 1.2 times the viscosity of the solvent; on the other hand, C_{18}TAB and C_{16}TAB are shear thinning in the same range. This is the sign of the viscoelasticity.
- Regime II (shear-thickening domain): except for C_{12}TAB and once the critical shear rate is reached, the three samples are shear thickening. The viscosity continuously increases to a maximum. The magnitude of the maximum is the same for C_{14}TAB and C_{16}TAB

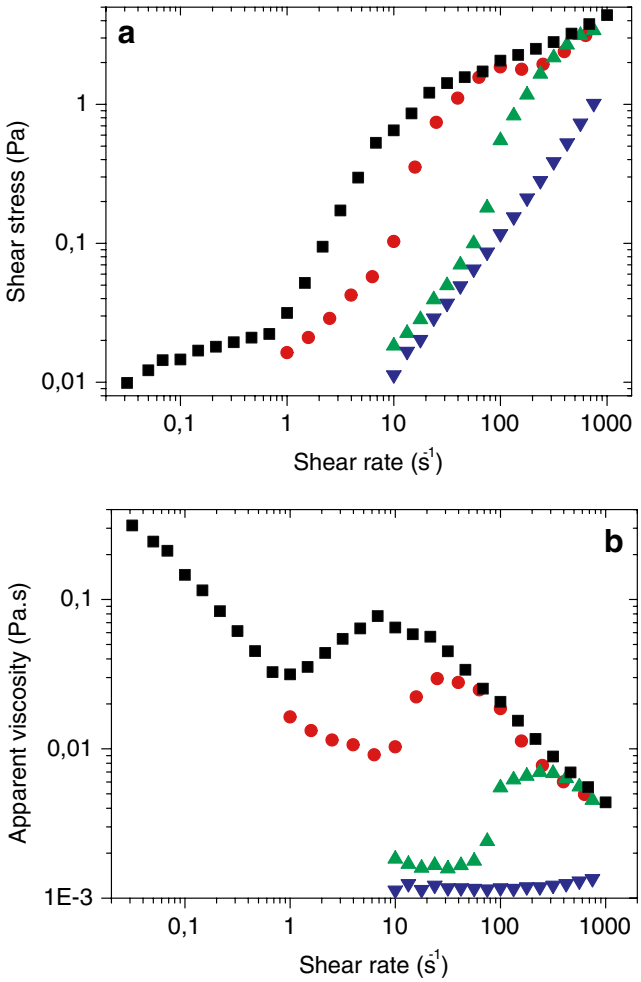

Fig. 6 Effect of the aliphatic chain length of the surfactant on the variations of shear stress (**a**) and apparent viscosity (**b**) for imposed shear rate for C_{18}TAB (*square*), C_{16}TAB (*circle*), C_{14}TAB (*triangle*) and C_{12}TAB (*inverted triangle*)

but smaller for C_{18}TAB. Could the entanglements already existing in regime I have an influence on the maximum reached by the viscosity? This still is an open question. However, a well-established result is that the length of the aliphatic chain reduces the value of the critical shear rates $\dot{\gamma}_c$ that are found to be 0.6, 6.0, and 36.9 s^{-1}, respectively, for C_{18}TAB, C_{16}TAB, and C_{14}TAB.

– Regime III (shear-thinning flow): Shear thinning occurs in the last region and in a log–log plot; η decreases vs the shear rate $\dot{\gamma}$ with the same slope for the three lengths. No sign of deterioration (bubbles, foam) were noticed even under high shear rates.

It is important to notice that the C_{12}TAB solution is newtonian. This is why, in the rest of this work, we will not investigate this system because we will focus our attention on the shear thickening.

Steady state flow in stress-controlled mode

When microscopic structural transitions are triggered by flow, the qualitative aspects of the flow curves are usually different under stress- and strain-controlled modes.

Figure 7 displays the variation of the stress and of the viscosity vs the shear rate in stress-controlled mode for C_{14}TAB, C_{16}TAB, and C_{18}TAB at 3 mM. The main difference in comparison to the strain-controlled mode appears in the shear-thickening domain; between a shear stress of 0.1 and 0.5 Pa for C_{18}TAB, the flow curve $\sigma(\dot{\gamma})$ has an S shape extending between 10 and 50 s^{-1} (see Fig. 7, empty rectangles) and is followed by a stress plateau. This S-shaped flow curve usually is associated with the coexistence of two or more bands stacked in the vorticity direction supporting the same shear rate but different shear stresses. C_{16}TAB has a nearly vertical evolution; while for C_{14}TAB, the flow curve increases smoothly with $\dot{\gamma}$ and only has a small curvature in the vicinity of 100 s^{-1}. The same

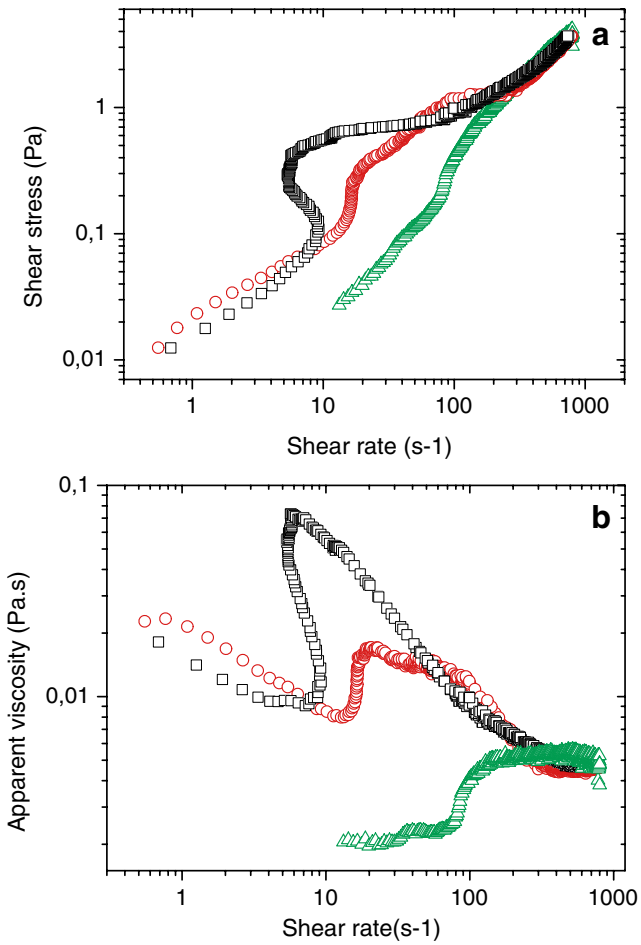

Fig. 7 Chain length effect on the variation of shear stress (**a**) and apparent viscosity (**b**) as a function of the shear rate for C_{18}TAB (*square*), C_{16}TAB (*circle*), and C_{14}TAB (*triangle*)

behavior can be observed in the curves of Fig. 7b when η is drawn vs $\dot{\gamma}$. Thus, operating in stress- or strain-controlled mode is not equivalent. The S-shaped flow curve of C_{18}TAB could be associated with stress-banded flows, a characteristic that does not appear in the strain-controlled flow curve. With the strain-controlled mode results, one can conclude that shear thickening exists in the three solutions, but the stress-controlled mode results bring more information, as one foresees that the distribution of the SIS in the gap may be different for the three samples, at least for C_{18}TAB and the group of C_{16}TAB and C_{14}TAB. A comparison between the data provided from two operating modes is made in Fig. 8 where the flow curves and the viscosity curves are drawn vs $\dot{\gamma}$.

It turns out that the width of the shear-thickening transition (regime II) and the flow in the other regions are not affected by the flow mode. We only note a change in the way the viscosity increases. This comparison shows that shear thickening takes place in a short range of shear rates in stress-controlled mode and with an S-shaped flow curve.

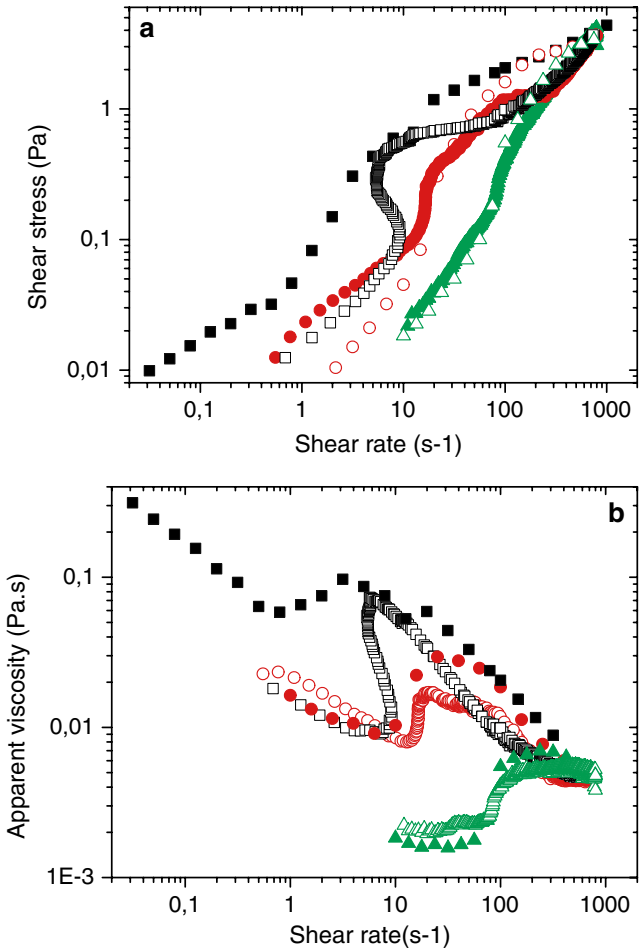

Fig. 8 Variation of the shear stress (**a**) and apparent viscosity (**b**) as a function of the shear rate: difference between strain-controlled mode, C_{18}TAB (*filled square*), C_{16}TAB (*filled circle*), and C_{14}TAB (*filled triangle*), and stress-controlled flow, C_{18}TAB (*open square*), C_{16}TAB (*open circle*), and C_{14}TAB (*open triangle*)

Rheo-optical flow under controlled shear rate

Rheo-optical flow experiments were performed on the three systems, C_{18}TAB, C_{16}TAB, and C_{14}TAB, in parallel to rheological investigations; this second optical technique is mainly used in the way to confirm the former results and to bring additional information about the evolution of the microstructure of the micellar arrangements under flow for surfactants with different chain lengths. We follow the variations of the extinction angle χ and of the retardation ϕ under controlled shear rate in the same strain ranges as in rheometry (the retardation φ is related to the birefringence intensity through the simple equation $\phi = \frac{2\pi e}{\lambda}\Delta n$). Experimental conditions identical to those used in rheometry are followed for each shear rate: The sample is subjected to flow during 600 s per point before any quantitative measurement; once the steady state has settled, the extinction angle χ and the retardation φ are measured. Figure 9 gather all these results and reports the variations of χ and Δn versus the shear rate $\dot{\gamma}$ for the three systems: C_{18}TAB, C_{16}TAB, and C_{14}TAB, respectively, in Fig. 9a, b, and c. The apparent viscosity η is also drawn in each figure to make the discussion easier; each rheological curve $\eta(\dot{\gamma})$ can be divided in three parts with different properties; in the low shear rates range (regime I), the sample behaves like a Newtonian fluid (C_{14}TAB) or is shear thinning (C_{18}TAB and C_{16}TAB); this first region is bounded on the right by a critical threshold $\dot{\gamma}_c$ where the shear-thickening transition is triggered; the viscosity η increases from a value close to the viscosity of the solvent to a maximum: this is regime II; finally, in the high shear rates range (regime III), the sample becomes shear thinning again, and the viscosity decreases. The overall aspect of the three curves is qualitatively the same: the angle χ drops to nearly zero when the shear thickening is triggered at the critical shear rate $\dot{\gamma}_c$ and remains close to this value in the whole range of $\dot{\gamma}$ and beyond $\dot{\gamma}_c$; the birefringence intensity variations reflect the same characteristics: in regime I, Δn is close to zero, sharply increases when $\dot{\gamma}$ reaches $\dot{\gamma}_c$, and tends to a plateau in regime III when η decreases again. This plateau behavior does not appear as clearly for C_{18}TAB as for C_{14}TAB because optical measurements are difficult and imprecise due to instabilities growing in the flow of C_{18}TAB; nevertheless, Δn does not decrease in regime III for the three surfactants. The principal conclusion of these observations is that shear thickening is accompanied by a nearly perfect alignment in the flow direction (χ=0) and a sharp increase of the birefringence intensity Δn. Such optical characteristics can only be achieved when strong structural

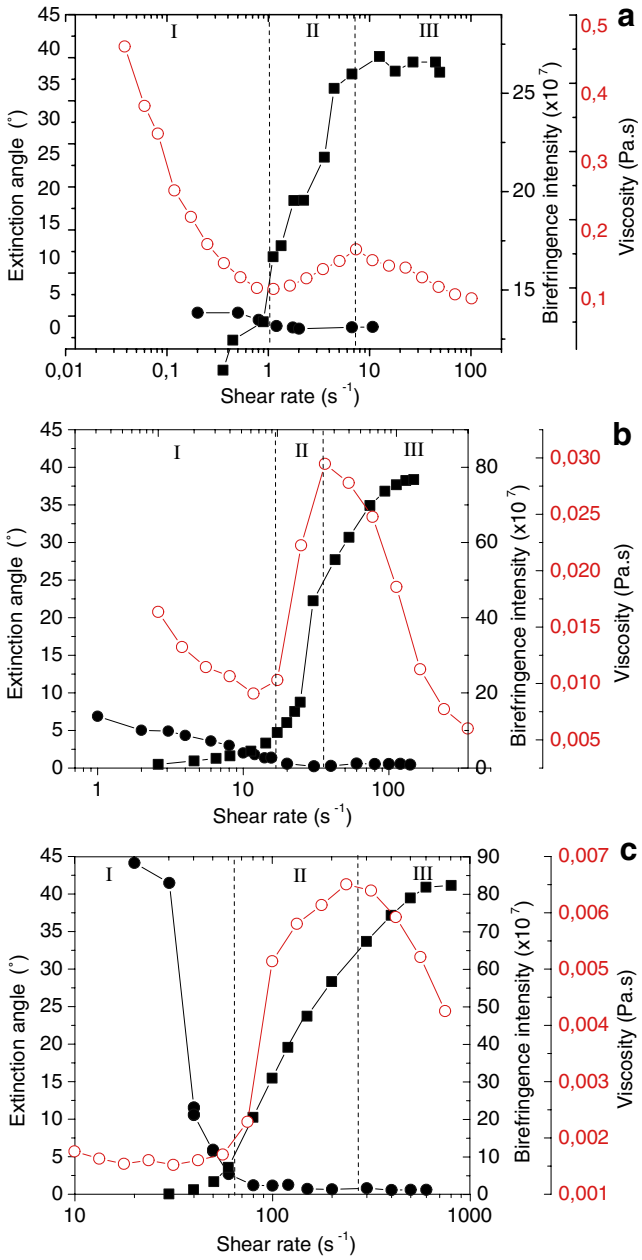

Fig. 9 Comparison between rheo-optic and rheometry in steady flow on the variation of the viscosity (*open circle*), birefringence intensity (*filled square*), and extinction angle (*filled circle*) as a function of the shear rate for C_{18}TAB (**a**), C_{16}TAB (**b**), and C_{14}TAB (**c**)

changes happen in the micellar arrangement. The alignment of long micelles in the flow direction has already been observed by Rehage et al. (1986), Wunderlich et al. (1987), and Hoffmann et al. (1991b); it is the consequence of the emergence of the SIS, but no details about its structure were given. We shall suggest an explanation for the shear-thickening transition leaning on our results and those provided by a recent study by Briels et al. (2004).

In most colloidal systems, shear thinning is explained by a better average orientation of the particles in the flow direction, and the longer the particles, the less energy necessary to keep the particles aligned in the flow direction. This is the conventional view of shear thinning, and the variations of χ and Δn vs $\dot{\gamma}$ in the low shear rate range fit well within this frame, so do C_{16}– and C_{18}TAB in regime I. However, the value of χ, only a few degrees, is all the more surprising under such weak flow conditions that the birefringence intensity remains rather weak; one must remember that the birefringence intensity is proportional to the concentration of anisotropic particles that is only about a few thousand ppm (3 mM); C_{14}TAB in regime I is slightly different: in the nearly Newtonian domain, χ is close to 45° but rapidly decreases to approximately 5° at the end of the Newtonian plateau.

Briels et al. (2004) have idealized a particle by a chain of micellar rings (Cates and Candau 2001; Head et al. 2002) that are stretched in the flow; this will bring the micelles closer and closer, and entanglements will be created (see the schematic entanglement associated with regime I in Fig. 10). Such a ring-like structure offers little resistance to the flow but can easily be oriented. Upon increasing the shear rate or stress, two entangled micelles will merge to form an H-structure with a micellar segment perpendicular to the stretching direction, i.e., to the flow direction. This small micellar segment will have a double action on the flow; it will prevent the solvent molecules from flowing between the parallel micelles but also prevent two worm-like micelles from freely slipping in parallel directions. These two phenomena may contribute to the increase of the apparent viscosity (see on Fig. 10, the H-micelle assumed to form in regime II). On further increasing the shear rate, η decreases again (regime III), but the angle χ remains close

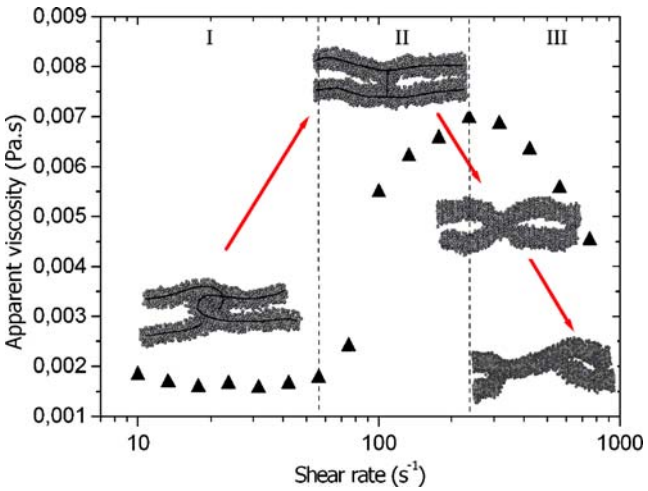

Fig. 10 Viscosity variation as a function of shear rate and micelles arrangements corresponding to each regime for C_{14}TAB system

to zero, and the birefringence intensity Δn still increases before slowly reaching a plateau value. The viscosity maximum does not seem to be correlated to the birefringence maximum. Referring again to the work of Briels et al. (2004), one can assume that the length of the bond joining two micelles decreases and finally disappear to leave an X structure that will gradually change into a 2Y micelle by sliding two branches of the X along the micelle body (see Fig. 10, the X and 2Y shapes associated with regime III). Such final arrangements will offer less resistance to the flow but will still confer a high degree of optical anisotropy to the fluid explaining the variation of Δn and χ in the high shear rate range.

Conclusions

We have investigated the influence of the aliphatic chain length on the rheological behavior of self-assembling molecules near and out of equilibrium. The shear-thickening transition observed is a typical characteristic of these dilute solutions, except C_{12}TAB, which remains Newtonian in the whole range of shear rates chosen for this survey. The magnitude of the phenomenon seems to be less pronounced when the flow is at first shear thinning in regime I. A definite qualitative correlation is found between the chain length and the critical shear rate. In the linear regime, the rheological behavior is the same in stress- or strain-controlled mode as expected. After the viscosity maximum, all the curves superimpose in the shear-thinning region (regime III) irrespective of the chain length, concentration, and flow modes. We can assume that the structural arrangement of the micelles is now the same in all the solutions. In the range of low shear rates, the qualitative aspect of the flow curve (Newtonian or shear thinning) clearly indicates that the length of the aliphatic chain has a strong influence on the micelles dimensions and arrangement. The overall behavior given by rheo-optics is in agreement with the rheometry data. As the chain length decreases, the system is less easily oriented in the flow direction and shows a lower birefringence intensity; this means a system with smaller micelles. Because the SIS formation results from the merging of micelles as a consequence of the energy brought by the shearing, we can expect that the macroscopic behavior will differ from one surfactant to another. Finally, we propose a physical explanation based on the results of computer simulation that predicts the evolution of the micellar arrangement out of equilibrium.

Acknowledgment We are grateful to Pr. W. J. Briels for allowing us to reproduce their drawings of the micellar arrangement.

References

Basu Ray G, Chakraborty I, Ghosh S, Moulik SP, Palepu R (2005) Self-aggregation of alkyltrimethylammonium bromides (C10-, C12-, C14-, and C16TAB) and their binary mixtures in aqueous medium: a critical and comprehensive assessment of interfacial behavior and bulk properties with reference to two types of micelle formation. Langmuir 21:10958

Boltenhagen P, Hu Y, Matthys EF, Pine DJ (1997) Inhomogeneous structure formation and shear thickening in worm-like micellar solutions. Europhys Lett 38:389

Briels WJ, Mulder P, den Otter WK (2004) Simulations of elementary processes in entangled wormlike micelles under tension: a kinetic pathway to Y-junctions and shear induced structures. J Phys Condens Matter 16:S3965

Cates ME, Candau SJ (2001) Ring-driven shear thickening in wormlike micelles? Europhys Lett 55:887

Decruppe JP, Hocquart R, Wydro T, Cressely R (1989) Flow birefringence study at the transition from the laminar to Taylor vortex flow. J Phys France 50:3371

Gamez-Corrales R, Berret JF, Walker LM, Oberdisse J (1999) Shear-thickening dilute surfactant solutions: equilibrium structure as studied by small-angle neutron scattering. Langmuir 15:6755

Hartmann V (1997) Contribution à l'étude expérimentale du rhéoépaississement et des transitions induites sous écoulements dans des solutions micellaires. PhD thesis, University of Metz

Head DA, Adjari A, Cates ME (2002) Rheological instability in a simple shear-thickening model. Europhys Lett 57:120

Hoffmann H, Hoffmann S, Rauscher A, Kalus J (1991a) Shear-induced transitions in micellar solutions. J Progr Colloid Polym Sci 84:24

Hofmann S, Rauscher A, Hoffmann H (1991b) Shear induced micellar structures. Ber Bunsenges Phys Chem 95:153

Hu Y, Rajaram CV, Wang SQ, Jamieson AM (1994) Shear thickening behavior of a rheopectic micellar solution: salt effects. Langmuir 10:80

Hu YT, Boltenhagen P, Matthys E, Pine DJ (1998a) Shear thickening in low-concentration solutions of wormlike micelles. I. Direct visualization of transient behavior and phase transitions. J Rheol 42:1185

Hu YT, Boltenhagen P, Matthys E, Pine DJ (1998b) Shear thickening in low-concentration solutions of wormlike micelles. II. Slip, fracture, and stability of the shear-induced phase. J Rheol 42:1209

Koch S, Schneider T, Küter W (1998) The velocity field of dilute cationic surfactant solutions in a Couette-viscometer. J Non-Newton Fluid Mech 78:47

Liu CH, Pine DJ (1996) Shear-induced gelation and fracture in micellar solutions. Phys Rev Lett 77:2121

Rehage H, Hoffmann H (1982) Shear induced phase transitions in highly dilute aqueous detergent solutions. Rheol Acta 21:561

Rehage H, Hoffmann H (1988) Rheological properties of viscoelastic surfactant systems. J Phys Chem 92:4712

Rehage H, Wunderlich I, Hoffmann H (1986) Shear-induced phase transitions in dilute aqueous surfactant solutions. Prog Colloid & Polym Sci 72:51

Swanson-Vethamuthu M, Almgren M, Karlsson G, Bahadur P (1996) Effect of sodium chloride and varied alkyl chain length on aqueous cationic surfactant-bile salt systems. Cryo-TEM and fluorescence quenching studies. Langmuir 12:2173

Wunderlich I, Hoffmann H, Rehage H (1987) Flow birefringence and rheological measurements on shear induced micellar structures. Rheol Acta 26:532